Tension Control and Force Estimation for Hybrid Drive Parallel Arm

Yasushi Mae, Tatsuo Arai and Kenji Inoue
Graduate School of Engineering Science, Osaka University,
1-3 Machikaneyama-cho, Toyonaka, Osaka 560-8531 JAPAN
mae@sys.es.osaka-u.ac.jp

Abstract

A hybrid drive parallel arm with 3 cylinders and 4 wires has been developed for manipulating heavy materials. This paper describes a tension control and estimation of external force for the hybrid parallel arm. The developed hybrid arm is a kind of actuation-redundant mechanism and its internal force can be freely controlled. The proposed algorithm will compensate the internal force, and estimate an external force working at handled object by exploiting 4 tension sensor data obtained at several arm positions. The basic experiments using the prototype arm are presented with external force estimation results.

1 Introduction

The high performance capabilities of manipulators, such as excellent repeatability, positioning accuracy and high speed, contribute to the automation in many industries as well as to increasing the factory productivity. A crane is a major handling tool for heavy materials in construction and shipbuilding fields. However, swing motion and rotation are generated and it is rather difficult to control them and to obtain accurate object positioning and orienting.

Wire drive mechanisms have advantages of producing large force and high speed due to its light weight, and there have been many researches on theory and applications [1]-[5]. Since the wire drive mechanism requires at least seven wires for full six degrees of freedom motion and they have to be located around a manipulated object, its workspace is entirely limited.

We have proposed a hybrid drive mechanism based on the mixture of high power wire (or cable) drive and cylinder actuation to obtain heavy duty manipulation in the application of automated handling and assembly in construction (**Fig.1**) [6, 7]. The tension of wire has to be maintained properly in the hybrid mechanism during its motion. Since the hybrid arm has actuation redundancy, the internal force may contribute to give proper tension in the wires with no disturbance of the end plate positioning. In manipulation, unpredictable external force may work at handled object especially in windy condition. The hybrid arm has 4 wires and their tensions have to be properly controlled even when unpredictable external force works at handled object to obtain precise manipulation.

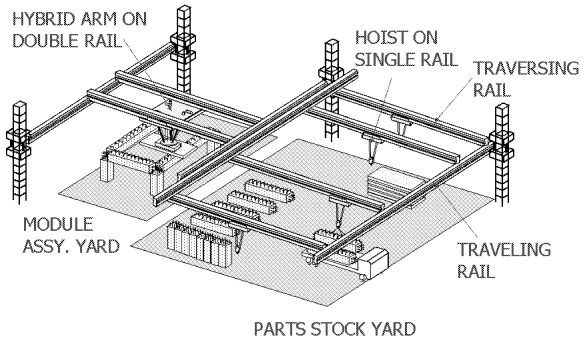

Figure 1: Assembly in construction

This paper describes a method of tension control by internal force compensation, and external force estimation from measuring by tension sensors attached to 4 wires. The wire tension sensor data enables to give the wires proper tension during its motion by exploiting this internal force[7, 8]. The sensor output is also utilized to estimate the external force and moment loaded on its end effector. Estimation of an external force works at some point of a handled object will enable us to use of the arm in windy condition.

2 Prototype hybrid drive parallel arm

2.1 Overview of the arm

We have proposed a hybrid drive parallel arm with wires and cylinders in order to design a compact han-

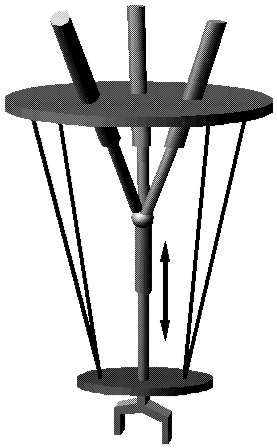

Figure 2: Configuration of hybrid drive parallel arm with variable rod

dling arm having its enlarged workspace. The main idea is to increase the limited workspace of the wire drive mechanism by replacing some wires with cylinders. Since the cylinder is capable of generating tension and compression, the actuators can be arranged on one side of a manipulated object, i.e. they do not have to surround the object as in the wire drive mechanism, and this enables the mechanism to enlarge its workspace. Six different types including the Stewart mechanism and an incomplete six wire mechanism have been analyzed and compared. Finally, we found that the three-cylinder/four-wire type (C3W4) with a variable connecting rod, shown in **Fig.2**, has good workspace in the application [6, 7, 8]. The variable rod has no actuator, but is passively moved by the wires and is fixed at its top and bottom end by a lock mechanism. This rod contributes to enlarge the arm workspace in the vertical direction. The rod is fixed at each end when the arm works for precise positioning and assembly.

2.2 Design of the prototype arm

A 1/7-scale prototype of hybrid drive parallel arm has been designed and built to confirm its applicability in heavy duty manipulation. In designing, automation in the construction of a middle scale apartment building is considered in our application. The main structures, floors and walls, are composed of a pre-casting concrete (PC) board with a size of 3×6×0.2[m] and a weight of 10[t]. The workspace of the arm is specified by the required motion in handling and assembling a PC board. It should be carried over 3[m] height

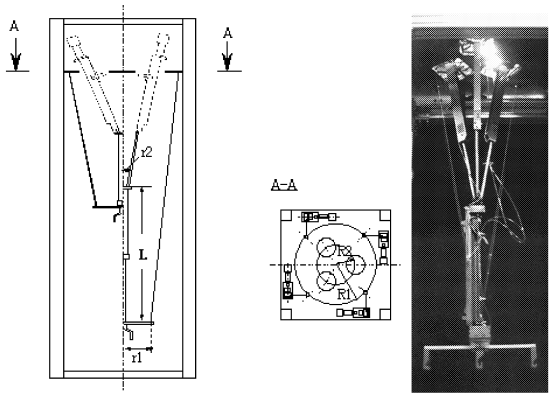

Figure 3: Mechanism drawing and overview of the prototype

Table 1: Optimum design parameters

	Length [m]		Length [m]
R_1	2.1	r_1	0.5
R_2	1.05	L	3.5-6.0

of one floor, then the workspace is specified to be a cylindrical volume with ϕ1×3.5[m]. Orienting motion is required in the assembling process, and its range should be over ±10[deg].

The workspace can be analyzed and compared by changing the link parameters, i.e. connecting points of wires and cylinders at the base plate, radius of the end plate, rod length, then the optimum values are selected to maximize workspace volume.

Fig.3 shows a mechanism drawing and overview of the prototype. Table 1 shows the selected parameters and **Fig.4** (a), (b) show the results of the angle of rotation at the top and the bottom length of the variable rod.

2.3 Tension Sensor

To give a wire proper tension, a certain tension sensor may be attached to a wire, then tension can be measured and it is fed back to keep desired tension by a servo mechanism. A servo may produce good quality of tension in the wire. The wire tension is measured by a tension sensor which can be easily attached to the wire. **Fig.5** shows a developed tension sensor. Wire tensions are measured by strain gage attached to the sensor.

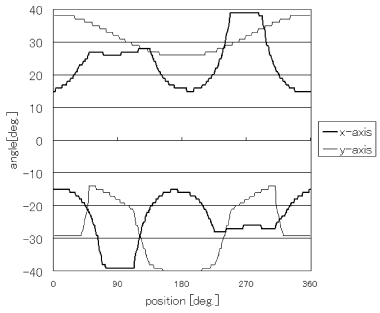

(a)Rotation angle at the shortest rod

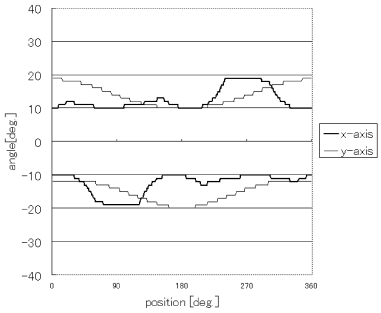

(b)Rotation angle at the longest rod

Figure 4: Maximum rotation angle in the workspace

3 Tension control for wire drive mechanism

3.1 Statics

A wire has just tension, not compression, and tension has to be controlled properly even in position control. The problem is the same as in our hybrid drive parallel arm, and tension of the four wires should be controlled so as not to lose the whole arm stiffness and to obtain fine positioning accuracy.

The relation between the output force $\boldsymbol{F}$(including moment) at the end plate and the wire tension and the cylinder force $\boldsymbol{\tau}$ is expressed as follows based on the statics as in the conventional parallel mechanisms [9],

$$\boldsymbol{F} = \boldsymbol{A}\boldsymbol{\tau}, \tag{1}$$

where $\boldsymbol{A}$ is the inverse of Jacobian matrix. $\boldsymbol{\tau}$ is derived from eq.(2) using $A^{\dagger}$, pseudo-inverse matrix of $\boldsymbol{A}$,

$$\boldsymbol{\tau} = A^{\dagger}\boldsymbol{F} + \left[I_7 - A^{\dagger}A\right]\boldsymbol{q}, \tag{2}$$

$$A^{\dagger} = A^T\left(AA^T\right)^{-1},$$

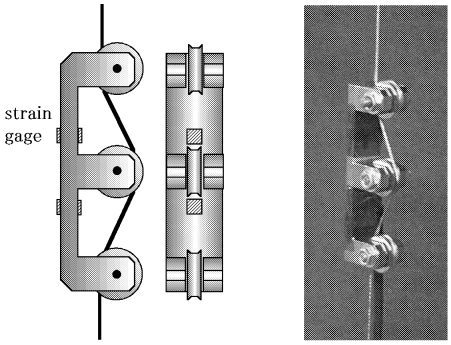

Figure 5: Tension sensor

where I_7 denotes an identity matrix, $\boldsymbol{q}$ denotes an arbitrary vector. Here, we introduce

$$\boldsymbol{F}_I = \left[I_7 - \boldsymbol{A}^{\dagger}\boldsymbol{A}\right]\boldsymbol{q}, \tag{3}$$

then,

$$\boldsymbol{\tau} = \boldsymbol{A}^{\dagger}\boldsymbol{F} + \boldsymbol{F}_I, \tag{4}$$

where $\boldsymbol{F}$ is the output force, and $\boldsymbol{F}_I$ is the internal force that has no effect on the output force. Proper tension can be obtained by adjusting $\boldsymbol{F}_I$.

The wires and the cylinders have the following conditions in their actuated force.

$$\begin{aligned} -M \le \left(A^{\dagger}\boldsymbol{F} + \boldsymbol{F}_I\right)_c \le M \qquad & (c : cylinder) \\ 0 \le \left(A^{\dagger}\boldsymbol{F} + \boldsymbol{F}_I\right)_w \le N \qquad & (w : wire) \end{aligned} \tag{5}$$

Inequality (5) has seven inequalities. And if $\boldsymbol{F}_I$ satisfies these seven simultaneous inequations, the proper force produced at each link can be obtained for control.

3.2 Tension Control by Internal Force Compensation

In the beginning, a tension is given to each wire not to slacken the wire. The initial tension and the link length including the initial link extension are set as references of the measurement of the tension and the link extension. The tension and the link extension from the references are denoted by $\boldsymbol{\tau}$ and $\Delta\boldsymbol{l}$, respectively. Then the link extension $\Delta\boldsymbol{l}$ is derived by the following equation.

$$\Delta\boldsymbol{l} = C\boldsymbol{\tau} = C(\boldsymbol{A}^{\dagger}\boldsymbol{F} + \boldsymbol{F}_I), \tag{6}$$

where C is a compliance matrix. The diagonal elements of C are compliances of cylinder and wire.

Table 2: Compensation of tensions

	$A^{\dagger}\boldsymbol{F}$		$\boldsymbol{F}_I$		$A^{\dagger}\boldsymbol{F}+\boldsymbol{F}_I$
cylinder1	2.08		-7.13		-5.05
cylinder2	-0.38		-5.62		-6
cylinder3	4.61		-8.68		-4.07
wire1	5.49	+	4.83	=	10.32
wire2	5.49		4.83		10.32
wire3	-0.03		5.87		5.84
wire4	-0.03		5.87		5.84

[kgf]

Table 3: Accuracy of repeat

standard deviation	x[mm]	y [mm]	z [mm]
without tension control	0.030	0.012	0.002
with tension control	0.012	0.009	0.001

In the prototype, the compliances of the wire and the cylinder are 1.84×10^{-2}[mm/N] and 3.36×10^{-6}[mm/N], respectively.

The inverse kinematics derives the desired link length $\boldsymbol{l}(t)$ at a time t. The internal force solved by equation (3) causes no motion of the end plate. By adjusting internal force $\boldsymbol{F}_I$, the forces $\boldsymbol{\tau}$ at link are controlled in order to satisfy the constraints (5). The corresponding link extension is denoted by $\Delta\boldsymbol{l}(t)$. Then the desired link length $\boldsymbol{l}'(t)$ is represented by

$$\boldsymbol{l}'(t) = \boldsymbol{l}(t) + \Delta\boldsymbol{l}(t). \tag{7}$$

By taking into account the wire extension $\Delta\boldsymbol{l}(t)$, we can give a desired end plate position and proper wire tension.

3.3 Example of Tension Control

One example of tension control is that the end plate is located at $(0, 100, 1300)[mm]$ with orientation of $(-5, 0, 0)[deg.]$, where two wires slacken in the minimal norm solutions($\boldsymbol{A}^{\dagger}\boldsymbol{F}$). The actual wire tensions are confirmed by measurement with the originally developed tension sensors. Table 2 shows the compensation with the calculated internal forces. By compensation of internal force wires 3 and 4 keep their proper tensions as well as other wires tensions properly.

Repeatability has been evaluated to confirm the stiffness of the whole arm. The repeatability with and without the compensation are compared by applying 30 trials in each x, y, and z direction. Table 3 shows these resultants and it represents that the tension control can contribute to improvement of positioning accuracy.

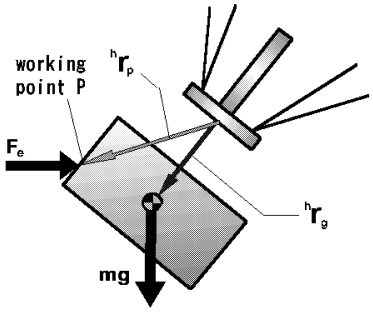

Figure 6: Arm hand and external force at working point

4 Estimation of External Force

The hybrid arm has only four tension sensors in its wires, and these outputs are not enough to derive the external force and moment loading on the arm end. Observing the arm statics carefully, it is possible to estimate the location of gravity center and the mass of a handled object with a number of wire tension measurements in different arm postures as long as they are stationary[10]. Using the same algorithm of [10], this section shows the estimation of the external force($\boldsymbol{F}_e$) at arbitrary point (not gravity center)(Fig.6). The external force can be looked upon as the force from any obstacle or from wind. In the following, algorithm will be derived for the external force estimation, and the computer simulation will confirm its validity. At last, the estimation error in experiments using the prototype of hybrid drive parallel arm is shown and evaluated.

4.1 Estimation algorithm

The arm statics is formulated from **Fig.6**. The force and moment at the arm hand from cylinder force and wire tension are as follows:

$$\begin{bmatrix} \boldsymbol{f}_h \\ \boldsymbol{m}_h \end{bmatrix} = A\boldsymbol{\tau} = \begin{bmatrix} A_c & A_w \end{bmatrix} \begin{bmatrix} \boldsymbol{\tau}_c \\ \boldsymbol{\tau}_w \end{bmatrix}. \tag{8}$$

$$\begin{array}{rcl} c & : & cylinder \\ w & : & wire \end{array}$$

$\boldsymbol{f}_h, \boldsymbol{m}_h$ are force and moment at the arm hand, $\boldsymbol{\tau}$ is

force at each link of the arm. $A \in R^{6\times 7}$ is an inverse Jacobian matrix and is divided into the following form by considering force and moment components.

$$A = \left[\begin{array}{cc} A_c & A_w \end{array} \right] = \left[\begin{array}{cc} A_{cf} & A_{wf} \\ A_{cm} & A_{wm} \end{array} \right] \tag{9}$$

The force and moment working at the arm hand are represented by

$$\left[\begin{array}{c} \boldsymbol{f}_h \\ \boldsymbol{m}_h \end{array} \right] = \left[\begin{array}{c} m\boldsymbol{g} + \boldsymbol{F_e} \\ R^h\boldsymbol{r}_g \otimes m\boldsymbol{g} + R^h\boldsymbol{r}_p \otimes \boldsymbol{F_e} \end{array} \right], \tag{10}$$

$$\otimes \quad : \quad vectorproduct$$

where m and ${}^h\boldsymbol{r}_g$ are mass and gravity point vector of a handled object. ${}^h\boldsymbol{r}_p$ is the vector of the external force at working point, and R is a rotational matrix relating the hand coordinate system to the base coordinate system.$\boldsymbol{F_e} \in R^{3\times 1}$ is the unknown external force against the arm hand.

Here the arm posture will be fixed at some point by keeping $\boldsymbol{F_e}$ constant. At i-th posture the following equations are obtained from eq.(8)(10) by defining skew symmetric matrices $S_p^{(i)} = R^{(i)h}\boldsymbol{r}_p\otimes, S_g^{(i)} = R^{(i)h}\boldsymbol{r}_g\otimes$.

$$\begin{array}{rcl} -I\boldsymbol{F_e} + A_{cf}^{(i)}\boldsymbol{\tau}_c^{(i)} & = & m\boldsymbol{g} - A_{wf}^{(i)}\boldsymbol{\tau}_w^{(i)} \\ -S_p^{(i)}\boldsymbol{F_e} + A_{cm}^{(i)}\boldsymbol{\tau}_c^{(i)} & = & S_g^{(i)}m\boldsymbol{g} - A_{wm}^{(i)}\boldsymbol{\tau}_w^{(i)}, \end{array} \tag{11}$$

where $\boldsymbol{F_e}$ and $\boldsymbol{\tau}_c^{(i)}$ are unknown, while $m, {}^h\boldsymbol{r}_g, \boldsymbol{\tau}_w^{(i)}$ are known variables. These equations are rewritten into the followings:

$$\left[\begin{array}{cc} -I & A_c^{(i)} \\ -S_p^{(i)} & \end{array} \right] \left[\begin{array}{c} \boldsymbol{F_e} \\ \boldsymbol{\tau}_c^{(i)} \end{array} \right] = \left[\begin{array}{c} m\boldsymbol{g} - A_{wf}^{(i)}\boldsymbol{\tau}_w^{(i)} \\ S_g^{(i)}m\boldsymbol{g} - A_{wm}^{(i)}\boldsymbol{\tau}_w^{(i)} \end{array} \right]. \tag{12}$$

If n times wire tension measurements are obtained at n postures, the total equations will be derived as follows:

$$\left[\begin{array}{ccccc} -I & A_c^{(1)} & \emptyset & \cdots & \emptyset \\ -S_p^{(1)} & \emptyset & \ddots & \ddots & \vdots \\ \vdots & \vdots & \ddots & \ddots & \emptyset \\ -I & & & & \\ -S_p^{(n)} & \emptyset & \cdots & \emptyset & A_c^{(n)} \end{array} \right] \left[\begin{array}{c} \boldsymbol{F_e} \\ \boldsymbol{\tau}_c^{(1)} \\ \vdots \\ \boldsymbol{\tau}_c^{(n)} \end{array} \right]$$

$$= \left[\begin{array}{c} m\boldsymbol{g} - A_{wf}^{(1)}\boldsymbol{\tau}_w^{(1)} \\ S_g^{(1)}m\boldsymbol{g} - A_{wm}^{(1)}\boldsymbol{\tau}_w^{(1)} \\ \vdots \\ m\boldsymbol{g} - A_{wf}^{(n)}\boldsymbol{\tau}_w^{(n)} \\ S_g^{(n)}m\boldsymbol{g} - A_{wm}^{(n)}\boldsymbol{\tau}_w^{(n)} \end{array} \right]. \tag{13}$$

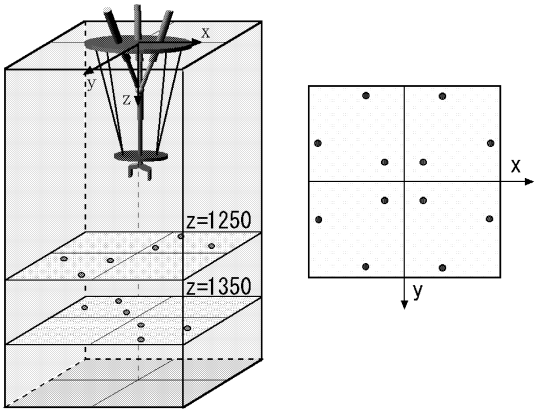

Figure 7: Measuring points

There are totally $(3+3n)$ unknown variables and $6n$ equations. Thus one measurement is enough to estimate unknown variables. If multiple measurements are available, the unknown variables are estimated by

$$\left[\begin{array}{c} \boldsymbol{F_e} \\ \boldsymbol{\tau}_c^{(1)} \\ \vdots \\ \boldsymbol{\tau}_c^{(n)} \end{array} \right] = \Gamma^\dagger \left[\begin{array}{c} m\boldsymbol{g} - A_{wf}^{(1)}\boldsymbol{\tau}_w^{(1)} \\ S_g^{(1)}m\boldsymbol{g} - A_{wm}^{(1)}\boldsymbol{\tau}_w^{(1)} \\ \vdots \\ m\boldsymbol{g} - A_{wf}^{(n)}\boldsymbol{\tau}_w^{(n)} \\ S_g^{(n)}m\boldsymbol{g} - A_{wm}^{(n)}\boldsymbol{\tau}_w^{(n)} \end{array} \right], \tag{14}$$

$$\Gamma = \left[\begin{array}{ccccc} -I & A_c^{(1)} & \emptyset & \cdots & \emptyset \\ -S_p^{(1)} & \emptyset & \ddots & \ddots & \vdots \\ \vdots & \vdots & \ddots & \ddots & \emptyset \\ -I & & & & \\ -S_p^{(n)} & \emptyset & \cdots & \emptyset & A_c^{(n)} \end{array} \right] \in R^{6n\times(3+3n)},$$

where $\Gamma^\dagger$ is a pseudo inverse matrix of Γ defined as follows:

$$\Gamma^\dagger = (\Gamma^T\Gamma)^{-1}\Gamma^T.$$

4.2 Experiments

In the experiment, external force is estimated from 12 measurements at different locations shown in **Fig.7**. The estimations have been obtained from the data by increasing the measurements from 1 to 12, one by one. The arm orientation at each point is changed at random within ± 10[deg] in xyz axes. The exact mass and center of gravity location of the object in the hand coordinates are 12.65[kg] and $(-17, -2, 247)$[mm], respectively.

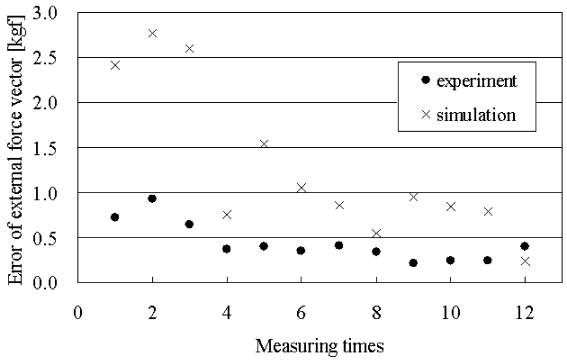

Figure 8: Estimation errors in external force vector

Estimation errors of the external force $\boldsymbol{F_e}$ are represented by black points in **Fig.8**. Although the estimation error decreases as the number of measurements increases, the final estimation error 0.4[kgf] still remains. This may be caused by low stiffness of the arm; the posture of the arm has shifted a little from ideal posture. For verification of the reason of these errors, possible errors are given to computer simulation intentionally, and their errors are compared. As possible errors, direction of external force and gravity center location are displaced $1[deg]$ and $2[mm]$, respectively. Black cross in **Fig.8** shows the estimation errors of the external force $\boldsymbol{F_e}$ in computer simulation. The estimation errors in computer simulation are worse than those in real experiments. Thus the remained errors may be caused by low stiffness of the arm.

In **Fig.8** some measuring points increase error, for example 2nd and 12th measurement. In these measurement, Γ, which depends only on the measurement posture of the arm, has a large condition number.

Thus the estimation quality depends not only on the stiffness but also on the measuring posture: position and orientation. Thus it is important for the estimation to select optimum measuring points.

5 Conclusions

The paper described a method of tension control by internal force compensation, estimation algorithm of external force at some working point using incomplete data from the tension sensors, as well as the control of force and moment for the new hybrid drive parallel arm. The estimation also works well and the basic experiments indicate a capability and applicability of the proposed method. It is also found that the estimation error is related to the arm stiffness and measurement points. The verification of measuring points is open to our future works.

References

[1] K.Homma and T.Arai :"Design of an Upper Limb Motion Assist System with Parallel Mechanism", Proc. of the IEEE Int. Conf. on Robotics and Automation, pp.1302-1307,1995.

[2] S.Kawamura,W.Choe,S.Tanaka,and S.R.Pandian : "Development of an Ultrahigh Speed Robot FALCON using Wire Drive System", Proc. of the IEEE Int. Conf. on Robotics and Automation, Vol.1,pp.215-220,1995.

[3] Landsberger,S.E.,and Sheridan, T.B. : "A new design for parallel link manipulators", Proc. of the 1985 IEEE International Conference of Systems,Man and Cybernetics,pp.812-814.

[4] Y.Shen, H.Osumi and T.Arai : "Set of Manipulating Forces in Wire-Driven Systems", Proc. of the IEEE/RSJ Int. Conf. on Intell. Robots and Systems, Vol.3,pp.1626-1631,1994.

[5] S.Tadokoro, S.Nishiok, aet al: "On Fundamental Design of Wire-Driven Parallel Manipulators With Redundancy", Proc. of the Japan/USA Symposium on Flexible Automation, 1, pp.151-158, 1996.

[6] T.Arai, K.Yuasa, et al: "Development of Hybrid Drive Parallel Arm for Heavy Material Hndring", Proc. of the 16th IAARC/IFAC/IEEE Int. Symposium on Automation and Robotics in Construction, pp.263-268, 1999.

[7] T.Arai, K.Yuasa, et al: "Hybrid Drive Parallel Arm For Heavy Material Handling",Proc. of the 1999 IEEE/RSJ International Conference on Intelligent Robots and Systems, pp.1234-1240, 1999.

[8] T.Arai, K.Yuasa, et al: "Hybrid Drive Parallel Arm and Its Motion Control",Proc. of the 2000 IEEE/RSJ International Conference on Intelligent Robots and Systems, pp.516-521, 2000.

[9] Robert S. Stoughton and T.Arai: "A Modified Stewart Platform Manipulator with Improved Dexterity",IEEE Transactions on Robotics and Automation,Vol.9,No.2,pp.166-172,1993.

[10] T.Arai, H.Kamishima, et al: "Tension Control and Its Application for Hybrid Drive Parallel Arm", 5th France-Japanese Congress of Mechatronics, pp.127-132,2001.